Combustion and Flame 160 (2013) 2396–2403

Contents lists available at SciVerse ScienceDirect

Combustion and Flame

journal homepage: www.elsevier.com/locate/combustflame

Studies on the stability limit extension of premixed and jet diffusion flames of methane, ethane, and propane using nanosecond repetitive pulsed discharge plasmas

Moon Soo Bak [a,*], Seong-kyun Im [a], M. Godfrey Mungal [b], Mark A. Cappelli [a]

[a] Mechanical Engineering Department, Stanford University, Stanford, CA 94305, United States
[b] School of Engineering, Santa Clara University, Santa Clara, CA 95053, United States

ARTICLE INFO

Article history:
Received 25 January 2013
Received in revised form 18 April 2013
Accepted 29 May 2013
Available online 28 June 2013

Keywords:
Plasma
Discharge
Combustion
Nanosecond
Breakdown

ABSTRACT

This paper examines the stabilization of premixed and jet diffusion flames of methane, ethane, and propane by nanosecond repetitive pulsed plasma discharges. Combustion products are measured using gas chromatography while laser-induced breakdown spectroscopy (LIBS) is used to characterize the local equivalence ratios. We find that in premixed flames, although plasma-assisted flame holding takes place under fuel-lean conditions, propagation of combustion occurs at/or above the known lean flammability limits. In jet diffusion flames, the flames are found to be anchored best to the discharge at jet speeds that are much higher than the normal blow-off speed when the discharge is placed where the local fuel–air equivalence ratio is in a limited flammable regime.

1. Introduction

Nanosecond repetitive pulsed discharges have been shown to stabilize premixed flames at fuel-lean conditions and diffusion flames at blow-off conditions [1]. Many researches have focused on the kinetics of this stabilization [2–7] and a significant radical production associated with gas heating at the plasma region is found to be responsible for an instantaneous combustion ignition process. The mechanism has been attributed to the quenching reactions of excited electronic states of species [7–10]. In particular, since molecular oxygen has a relatively weak bonding, it can be dissociated during the quenching process and the produced energetic atomic oxygen can quickly raise the gas temperature. In low pressure experiments, the role of direct radical production was apparent because the temperature rise was found to be negligible [3]. However, in higher pressure studies (e.g., atmospheric pressure), the stabilization was obtained when the discharge is in a filamentary mode, which is accompanied by a significant temperature rise [4–7].

An extension of the lean flammability limit of premixed flames with pulsed plasmas has been demonstrated for a range of pressures [3] and plasma powers [4–6,11]. However, few studies quantify this extent by analyzing final combustion products [11]. In previous studies, we carried out gas chromatography measurements for methane premixed flames and found that while visible evidence for the stabilization is apparent with the application of these pulsed discharges, the extension of efficient combustion beyond the known lean flammability limit is not significant when the discharge plasma power (typically a few tens of Watts) is relatively small in comparison to the combustion power (which is typically a few kilo-Watts) [7]. In this paper, we have extended our previous study to other small hydrocarbons (ethane and propane) to verify that the propagation of combustion induced by the discharge in fact occurs at the known lean flammability limit.

Research on the use of pulsed discharge stabilization of jet diffusion flames has been relatively rare. The stabilization of methane jet flames and propane jet flames with the use of repetitive pulsed plasmas were reported by Kim et al. [12,13] and Criner et al. [14], respectively. The ignition of hydrogen or ethylene jets in a supersonic crossflow configuration with nanosecond pulsed discharges was reported by Do et al. [15,16]. The results of Ref. [12] for methane jet flames in a subsonic coflow conditions showed that for effective flame stabilization, the discharge must be placed in a region within the mixing layer where there exists a critical fuel–air ratio. They defined a flame emission-based duty-cycle to quantify the extent of combustion and mapped the local fuel–air ratio using plasma-induced breakdown spectroscopy. We revisit the study of nanosecond pulsed plasma stability of jet diffusion flames for methane and other small hydrocarbon fuels (ethane, and propane)

* Corresponding author.
E-mail address: moonsoo@stanford.edu (M.S. Bak).

0010-2180/$ - see front matter © 2013 The Combustion Institute. Published by Elsevier Inc. All rights reserved.
http://dx.doi.org/10.1016/j.combustflame.2013.05.023

but with quantitative measurements of combustion products close to the flame tip using gas chromatography. In addition, the fuel–air ratio at the discharge placement is measured using the well-studied method of laser-induced breakdown spectroscopy (LIBS) [17].

2. Experimental setup

Schematics of nanosecond repetitive pulsed discharge-stabilized premixed and jet diffusion flame experiments are shown in Fig. 1a and b, respectively. The discharges are generated between two tungsten electrodes of 1 mm diameter separated vertically by 1 mm (parallel to the streamwise direction) in order to minimize the effect of ionic wind on the flow field and combustion. High voltage pulses, 9 ns in pulse width, are applied using a pulse generator (FID Technology F1112) in the premixed (8 kV peak voltage) and diffusion (9 kV peak voltage) flame configurations, respectively. The pulse repetition rate is varied between 10 kHz and 50 kHz for the premixed flame studies whereas it is fixed at 30 kHz for the diffusion flame studies. An upper limit for the total power deposited into the plasma is obtained from the measured direct-current power delivered to the pulsed power supply. For the premixed combustion cases, this varied between 5 W to 24.4 W (as the repetition rate varies from 10 kHz to 50 kHz). It is noteworthy that this upper limit is still very small in comparison to the rate of heat release by combustion (if it is complete), which is 870–1260 W (over the range of equivalence ratio studied). For the jet diffusion flame studies, the upper limit in deposited power is 18 W, again, relatively small in comparison to the rate of heat release, which can be between 5600 W and 14800 W.

In the premixed flame studies, fuel (methane, ethane, or propane) is premixed with air and the mixture flows upward though a 44 mm inner diameter quartz tube. The discharge location is placed 1 mm above the tube to avoid air entrainment into the flow. The fuel–air ratio is controlled using mass flow controllers (Unit UFC-3020A for air, and MKS 247A for small hydrocarbon fuels) that are calibrated against a dry test meter (Elster American Meter

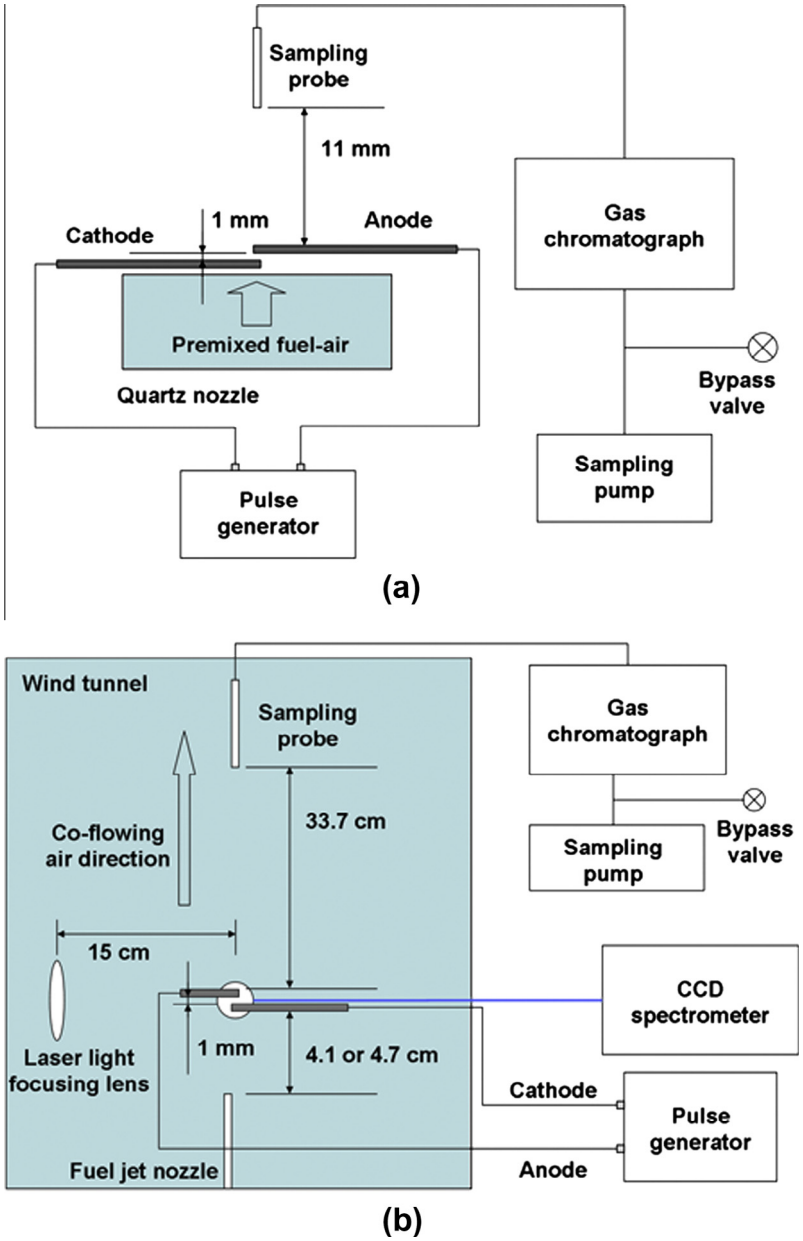

Fig. 1. Schematics of nanosecond repetitive pulsed discharge-stabilized (a) lean premixed flame and (b) diffusion jet flame experiments.

DTM-200A). The fuel–air equivalence ratio is varied over the fuel-lean range of between 0.42 and 0.61, and the total flow speed is set to be about 42.5 cm/s.

The diffusion flame studies are conducted in a 50 cm by 50 cm cross-sectional vertical wind tunnel. A downstream 1.5 hp blower induces a flow in an upward direction and a fuel jet is injected parallel to the flow. The inner diameters of fuel jet nozzles are set to be 2.16 mm, 1.85 mm, and 1.58 mm for methane, ethane, and propane, respectively. Different nozzle diameters are used to produce flames of relatively similar size. The fuel jet flow rates are controlled using a mass flow controller (Brooks 5850E) also calibrated for each of the fuels using the dry test meter. The fuel jet nozzle speeds are varied between 43.0 m/s ($Re_D = 5400$) and 103 m/s ($Re_D = 13000$) for methane, 41.0 m/s ($Re_D = 9800$) and 85.6 m/s ($Re_D = 20600$) for ethane, and 34.3 m/s ($Re_D = 11900$) and 81.0 m/s ($Re_D = 28100$) for propane while the coflow speed is fixed at 0.8 m/s. The discharge is placed 41 mm, 41 mm, and 47 mm downstream from the jet nozzle for methane, ethane, and propane, respectively. The discharge location could be moved along the radial direction using a translational stage.

Gas chromatography is carried out to analyze combustion products. Samples are directed to a gas chromatograph (Varian Inc.) equipped with Porapak Q and Molsieve 5 Å columns using a small-size vacuum pump (Thermo Scientific 420-1901). A bypass valve attached to the inlet port of the pump is adjusted to allow the suction speed at the tip of the sampling probe similar to the flow speed. Porapak Q column is used to separate H_2, air, CH_4, CO, CO_2, C_2H_4, C_2H_6, C_3H_6, and C_3H_8, and Molseive 5 Å is used to separate air into O_2 and N_2. The species concentrations are detected using both a thermal conductivity detector (TCD) (resolution below 1% in mole fraction) and a pulsed discharge helium ionization detector (PDHID) (resolution below 100 ppm). The sampling probes, centered along the nozzle axis, are placed 11 mm and 33.7 cm downstream from the discharges for the premixed flames and diffusion flames, respectively.

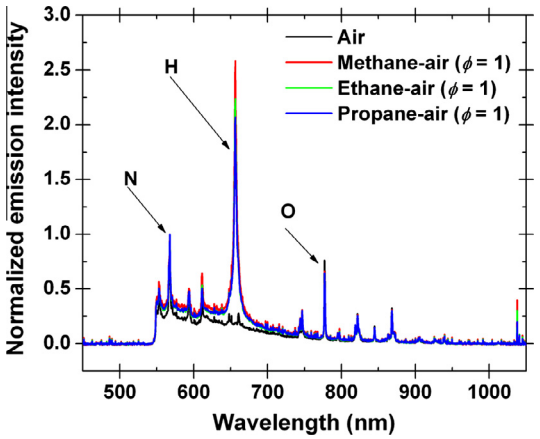

Fig. 2. Example of laser breakdown emission spectrum in air and in methane–air, ethane–air, and propane–air at unity equivalence ratio.

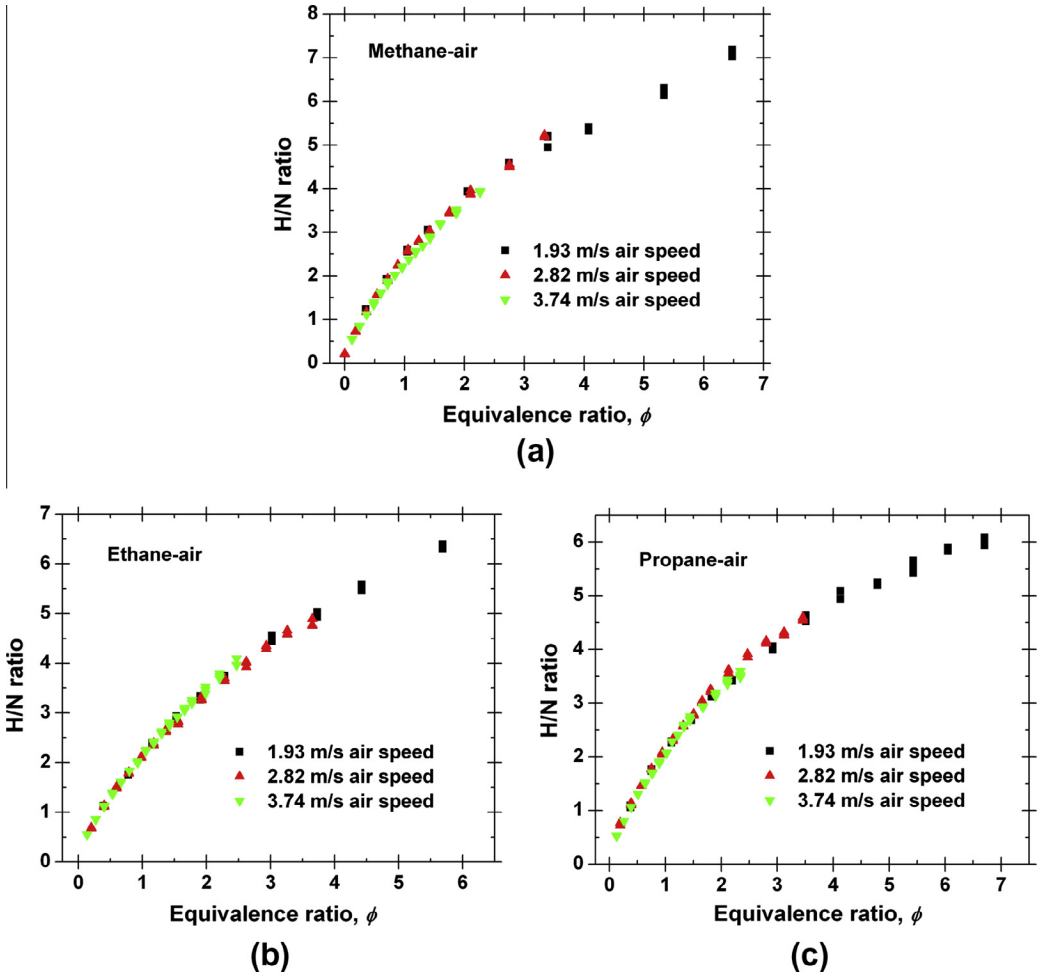

Fig. 3. Mapping between H/N spectral line intensity ratio and equivalence ratio of (a) methane–air, (b) ethane–air, and (c) propane–air mixtures.

LIBS is carried out in the jet diffusion flame experiment to obtain local equivalence ratios. For the LIBS measurements we employ a Nd:Yag laser (Spectra Physics PIV-400) operated at 15 Hz, with the 8 ns (FWHM) pulse frequency-doubled 532 nm focused to a tight beam waist using a 15 cm focal length lens. The breakdown emission is spectrally filtered with a long-pass filter (onset of transmission at 550 nm, Thorlabs FEL 0550) to block the 532 nm line of the laser and collected by a collimating lens for coupling into a collection optical fiber. The optical placement is adjusted to capture the central spot of the breakdown kernel, the spectrally broad signature of which forms a continuous background against the relatively discrete structure of the molecular and atomic spectral lines. The emission is analyzed using a compact charge-coupled device (CCD) spectrometer (Ocean Optics S2000) set to integrate over time, the emission generated from 21 laser breakdown events. The entire laser focusing and emission collection optics shares a common translation stage with the electrodes, allowing the LIBS measurement to be made at the same location of the nanosecond pulsed discharge excitation. To calibrate the LIBS spectrum, we carry out the LIBS study in a flow of a known fuel–air mixture. The source for this mixture is a premixed burner (10 mm diameter nozzle) with varying fuel–air mixtures and air flow speeds of 1.93 m/s, 2.82 m/s, and 3.74 m/s. These speeds are chosen such that flames initiated by the LIBS process do not attach to the burner (i.e., they are anchored at the breakdown point). It is important that the flame does not propagate down to the burner surface so that the composition of the flow before the next LIBS pulse is an unburnt fuel–air mixture. In these calibration studies, the fuel and air flow rates are also controlled using mass flow controllers (Brooks 5850E for fuel). The breakdown location is placed adjacent to the nozzle exit plane to minimize dilution of the known equivalence ratio flow by the surrounding air.

3. Laser induced breakdown spectroscopy

The laser breakdown emission spectrum in air and methane–air, ethane–air, and propane–air mixtures at unity equivalence ratio are shown in Fig. 2. The spectra are normalized to the strength of the 567.956 nm atomic nitrogen (N) spectral line. We find that while the Balmer alpha (H_α) spectral line intensities of atomic hydrogen (H) are not equal for the different fuels at a given equivalence ratio, they are proportional to the equivalence ratio. The H/N spectral line intensity ratio is calibrated against varying equivalence ratio, ϕ, from fuel-lean ($\phi \approx 0$) to fuel-rich ($\phi \approx 6.5$) conditions for methane–air, ethane–air, and propane–air mixtures. During the experiment, the laser power is kept constant at 0.330 ± 0.015 W (22 ± 1 mJ per pulse). The relationships between the H/N ratio and the equivalence ratio for the three mixture types are shown in Fig. 3a, b, and c, respectively. This calibration is

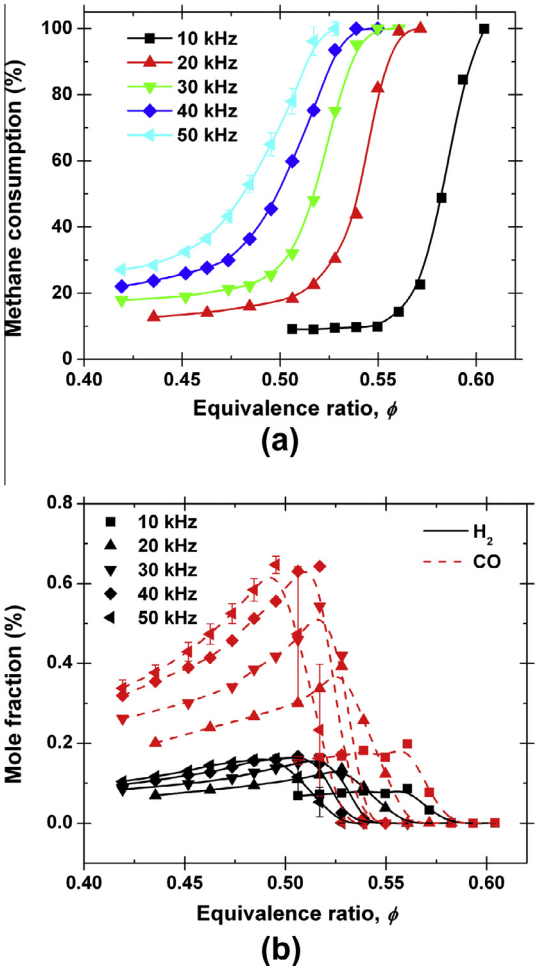

Fig. 4. (a) Methane consumption and (b) H_2 and CO mole fractions as a function of discharge repetition rate at 11 mm fixed downstream location from the discharges.

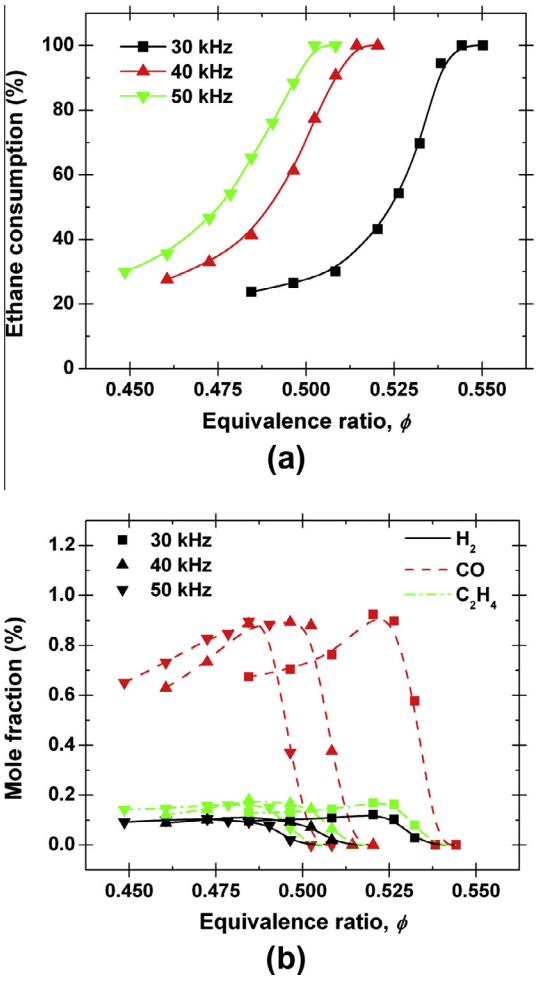

Fig. 5. (a) Ethane consumption and (b) H_2, CO, and C_2H_4 mole fractions as a function of discharge repetition rate at 11 mm fixed downstream location from the discharges.

carried out for three different flow rates, and the H/N ratio is found to be independent to the flow speed. We also find that the ratio is independent of laser power over a limited range spanned by shot-to-shot fluctuations in laser power (about 10% of the laser power). These calibrations are used to obtain the local equivalence ratio during studies of plasma-assisted stabilization in jet diffusion flames.

4. Lean flammability limit extension

The fuel consumption is defined here as:

$$\eta = \frac{X_{\text{fuel},i} - X_{\text{fuel}}}{X_{\text{fuel},i}} \times 100 \quad (1)$$

Here $X_{\text{fuel,i}}$ and X_{fuel} are the initial and local fuel mole fractions, respectively. We use this as a measure of the extent of combustion (i.e., combustion efficiency) when analyzing the effectiveness of nanosecond pulsed plasmas in stabilizing premixed flames.

Combustion products of pulsed discharge-stabilized lean premixed methane–air, ethane–air, and propane–air are analyzed. Figures 4a, 5a, and 6a show the fuel consumptions as a function of equivalence ratio for different discharge repetition rates between 10 kHz and 50 kHz. We note that no combustion is achieved without the discharges at all of the tested conditions. For methane–air, we experience plasma-assisted stabilization for all of the tested repetition rates although its extent was more significant with the increased rates. The equivalence ratio for complete combustion is found to decrease from 0.605 at 10 kHz to 0.53 at 50 kHz. For ethane–air, we could not see a continuous combustion stream for any of the tested equivalence ratios for 10 kHz and 20 kHz. The flame was intermittent and the combustion products were almost unburnt in a time-averaged sense. The equivalence ratio for complete combustion is found to decrease from 0.544 at 30 kHz to 0.503 at 50 kHz. For propane–air, repetition rates beyond 30 kHz are required for obtaining a stable combustion stream. The equivalence ratio for the complete combustion is found to decrease from 0.56 at 40 kHz to 0.54 at 50 kHz. It is apparent that the discharges are able to flame-hold under very fuel-lean conditions. However, the threshold ratios for complete combustion at locations downstream of the discharges are found to be very close to the known lean flammability limit (0.53, 0.52, and 0.54 for methane–air, ethane–air, and propane–air mixtures [18]). It is noteworthy that gas chromatograph measurements along a streamwise direction that we reported in a prior study for methane–air flames [7] showed that the combustion initiated by the discharges is gradually quenched at downstream discharge locations when the combustion of the mixture is not sustainable (i.e., when the equivalence ratio is not above the known lean flammability limit). In essence, the extent of combustion relies on the propagation of the flame. This conclusion was also obtained by Pancheshnyi et al. [5], who reported on studies of discharge pulse ignition in a static cell that if the initial discharge ignites a diluted fuel–oxygen mixture, the subsequent pulses seem to have little effect on the combustion process.

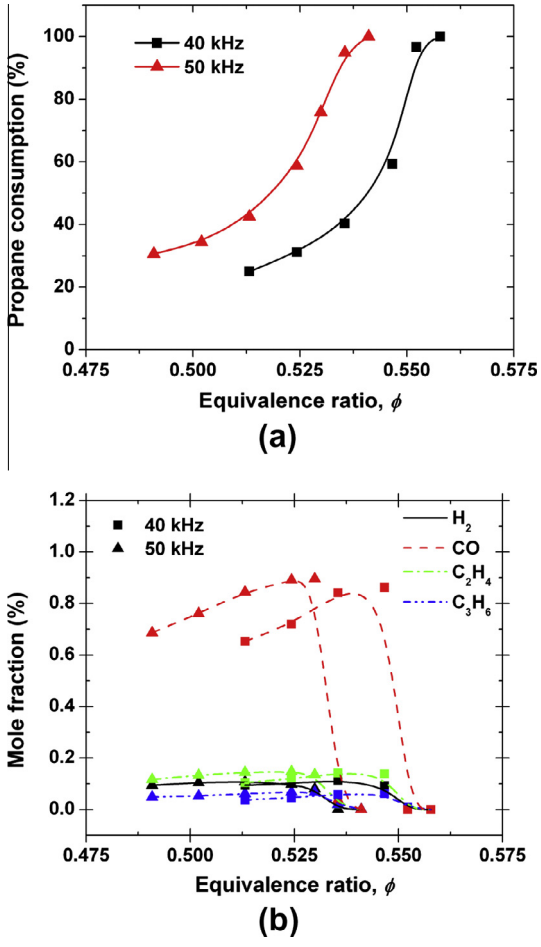

Fig. 6. (a) Propane consumption and (b) H_2, CO, C_2H_4, and C_3H_6 mole fractions as a function of discharge repetition rate at 11 mm fixed downstream location from the discharges.

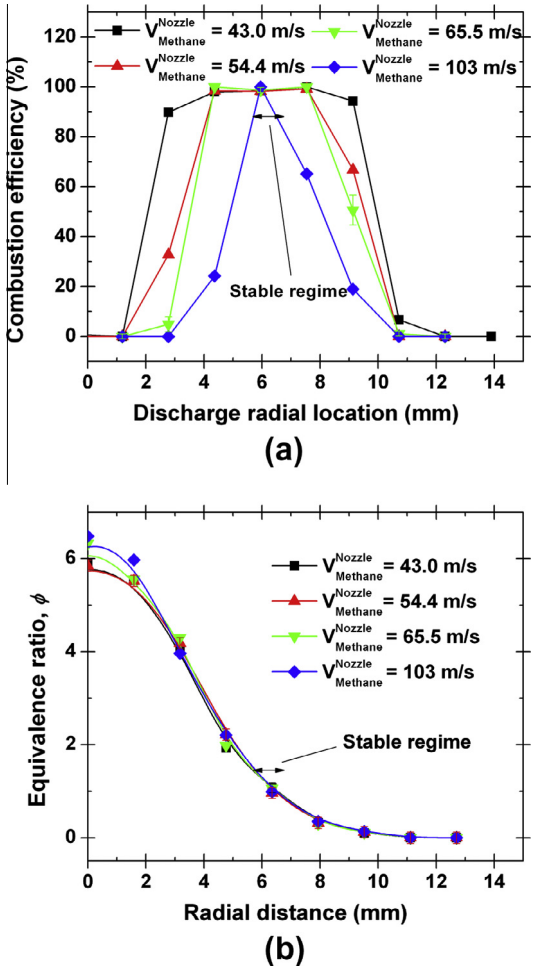

Fig. 7. (a) Methane jet combustion efficiencies at a fixed axial downstream location given radial discharge locations and (b) the corresponding equivalence ratios at the discharge locations.

The concentrations of the incomplete combustion products such as H_2 and CO for methane as well as C_2H_4 for ethane, and C_3H_6 for propane are plotted as a function of equivalence ratio for different discharge repetition rates between 10 kHz and 50 kHz for methane–air, ethane–air, and propane–air in Figs. 4b, 5b, and 6b, respectively. While trace levels of CH_4 are also measured for the ethane–air and propane–air combustion cases, they are not shown in the figures because they were lower than the quantitative detection limit. When the equivalence ratio is below the limit for complete combustion, the partial products produced during the quenching of combustion (initiated at the discharge region) increase as the equivalence ratio increases for all of the fuels and repetition rates. When the equivalence ratio reaches that for complete combustion, these partial products are converted to H_2O and CO_2. This finding indicates that the combustion is self-sustainable only when the equivalence ratio is above a critical limit which is found to be very close to the known flammability limits for all of the fuels studied.

5. Blow-off limit extension

Studies of the stabilization of methane, ethane, and propane jet diffusion flame with nanosecond repetitive pulsed discharges are also carried out. At a coflow air speed of 0.8 m/s, a methane jet flame is not stable in the absence of a discharge (i.e., always experiences blow-off irrespective of the jet speed). We find that ethane and propane jet flames experience blow-off at nozzle speeds of 38.5 m/s and 32.0 m/s, respectively. To account for the effect of the presence of the electrodes on the blow-off speed, these limits were measured in the presence of the electrodes. All of the tested nozzle speeds for these stabilization studies are set to be faster than the observed blow-off speeds. When stabilized by the discharge, the combustion efficiency is defined here as:

$$\eta = \frac{X_{CO_2} + X_{CO}}{\sum_{j=\text{species}} \alpha_{\text{carbon},j} X_j} \times 100 \qquad (2)$$

Here X_j is the local mole fraction of species j at the sampling location and $\alpha_{\text{carbon},j}$ is the containing carbon number of species j.

The combustion efficiencies (measured at fixed axial downstream location while varying the discharge radial placement) and the corresponding equivalence ratios at the discharge locations, for methane, ethane, and propane flames, are shown in Figs. 7a and b, 8a and b, and 9a and b, respectively. The radial variations in the equivalence ratio are found to be smooth and somewhat independent of the jet speeds studied. We note that the measured ratio is a time-averaged value and fluctuations are not accounted for. No combustion (stabilization) is seen when the discharge is located where the fuel concentration is too rich (towards the jet axis) or too lean (large radial locations) for all three types of fuels. The flames are found to be anchored best to the discharge (i.e., not pulsating) when the discharge is placed where the local equivalence ratio, ϕ, is between 0.8 and 1.9 (in the most "stable

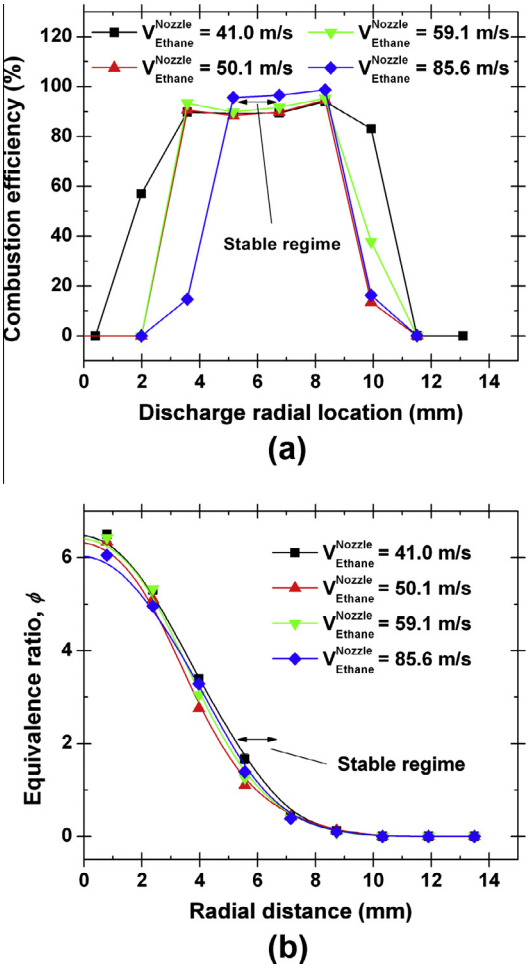

Fig. 8. (a) Ethane jet combustion efficiencies at a fixed axial downstream location given radial discharge locations and (b) the corresponding equivalence ratios at the discharge locations.

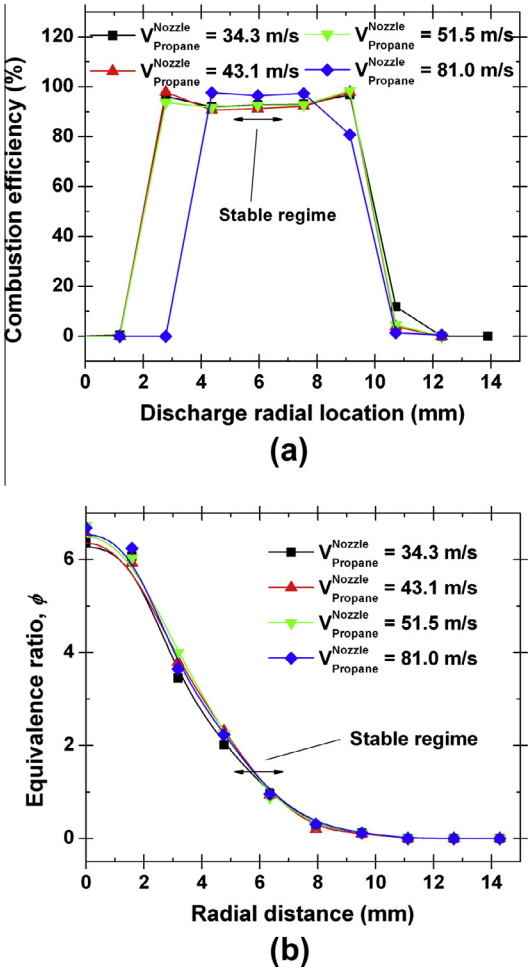

Fig. 9. (a) Propane jet combustion efficiencies at a fixed axial downstream location given radial discharge locations and (b) the corresponding equivalence ratios at the discharge locations.

regime"), i.e., where the mixtures are close to a combustible condition (this regime is marked in the figures). When the discharge is placed in a region where ϕ is outside of this range, the flame base pulsates with diminishing frequency. In spite of this pulsation, complete combustion is still achieved when close to the stable regime because of its high pulsation frequency. Therefore, the spatial regions of complete combustion are found to be broader than those for stable flames. However, these regions of complete combustion become narrower as the jet speed increases for all of the tested fuels. For example, we see that for the case of methane, a jet speed of 103 m/s results in complete combustion only within a narrow spatial region that overlaps the region of flame stability.

We can define the element selectivity of a particular molecule as the probability (between 0 and 1) that the element's fate during combustion is to form that molecule as quantified by downstream gas chromatography. The C and H selectivities of the measured combustion products at a fixed axial downstream location while varying the discharge radial locations for methane, ethane and propane jets are shown in Figs. 10a and b, 11a and b, and 12a and b, respectively. Since H_2O is removed by the desiccant before entering the gas chromatograph, its concentration is instead calculated by an element balance. We find that C and H are converted mostly to CO_2 and H_2O around the stable flame regimes. However, interestingly, the stable partial products of H_2 and CO for the methane jet, and H_2, CO, CH_4, and C_2H_4 for both ethane and propane jets

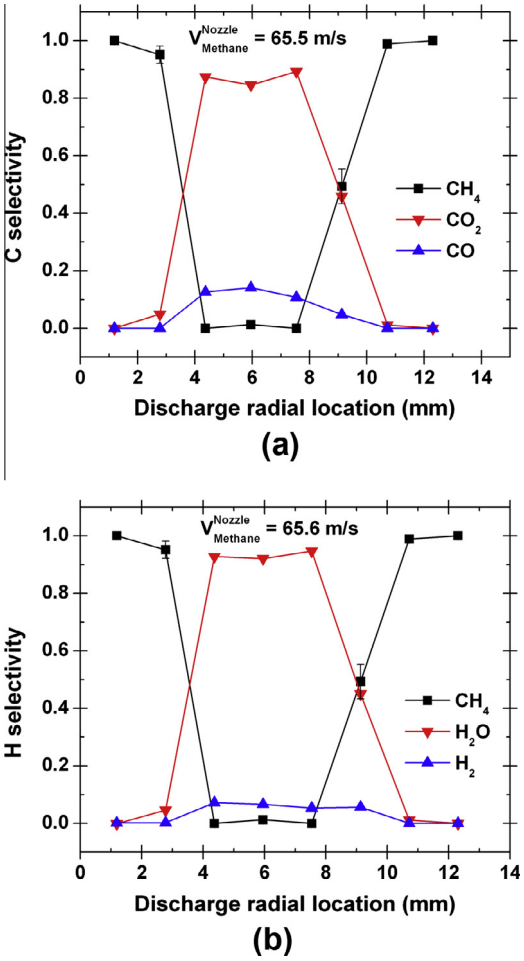

Fig. 10. (a) Carbon selectivity and (b) hydrogen selectivity of combustion products for discharge-stabilized methane-jet diffusion flame with varying discharge radial locations at the conditions that the nozzle speed is 65.5 m/s and the coflow speed is 0.8 m/s.

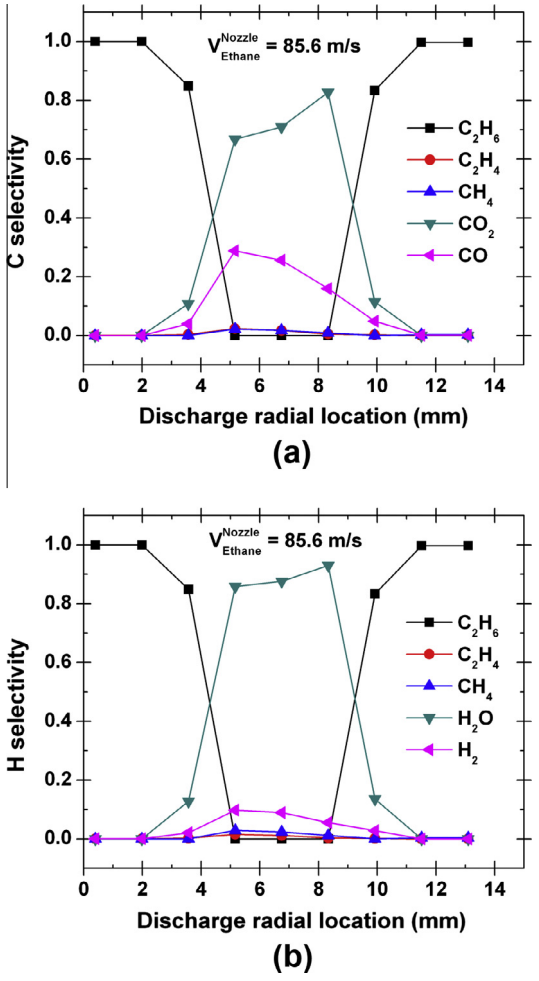

Fig. 11. (a) Carbon selectivity and (b) hydrogen selectivity of combustion products for discharge-stabilized ethane-jet diffusion flame with varying discharge radial locations at the conditions that the nozzle speed is 85.6 m/s and the coflow speed is 0.8 m/s.

peak in the stable regimes. We attribute this to the elongation of the flame in this regime. Outside of this stable regime, combustion was intermittent rather than producing a continuous stream of incomplete combustion and the pulsation during combustion leads to an apparent shortening of the flame length. This is to be expected since during the times when the flame is non-burning, the jet entrains significantly more air which would lead to flame shortening [19].

Figure 13 is a photograph of a discharge-stabilized propane-jet diffusion flame under conditions that the discharge is located in a region where ϕ is about 1.27 and a propane jet speed is 43.1 m/s. The flame is attached to the discharge and the flame appears steady. One can see that combustion is initiated at the discharge kernel (bright spot in the foreground of the flame base) and subsequently propagates downstream along the contour where we presume ϕ is close to 1. The flame base loop is found to be thicker because it branches out towards both fuel-lean and fuel-rich sides, forming a triple flame. Under stabilized conditions marked as the stable regime in Figs. 7–9, the flame has more of a resemblance to a turbulent diffusion flame with an obliquely cut base, rather than that of a lifted turbulent flame, see [20].

6. Conclusion

Lean premixed flames and jet diffusion flames for three different fuels of methane, ethane, and propane were stabilized with

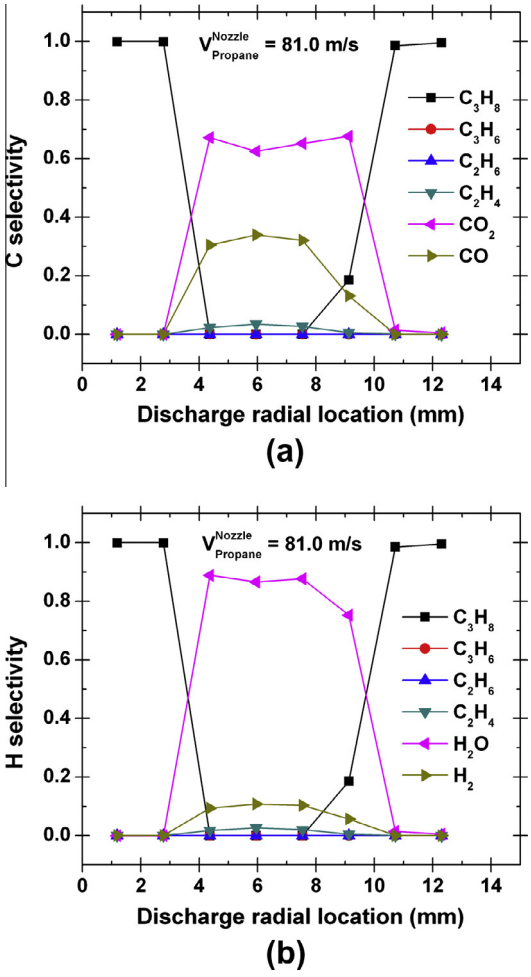

Fig. 12. (a) Carbon selectivity and (b) hydrogen selectivity of combustion products for discharge-stabilized propane-jet diffusion flame with varying discharge radial locations at the conditions that the nozzle speed is 81.0 m/s and the coflow speed is 0.8 m/s.

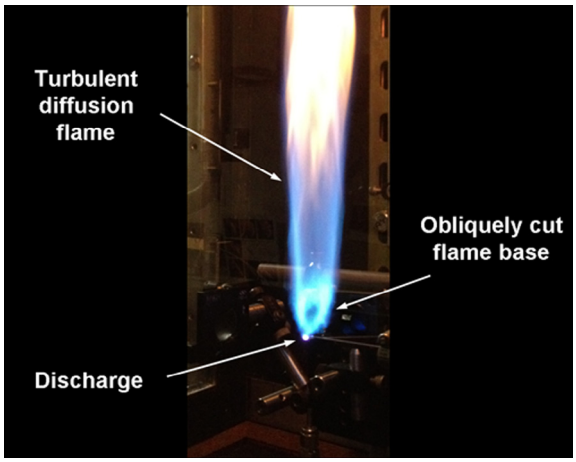

Fig. 13. Photograph of discharge-stabilized propane-jet flames at the condition that the discharges locate where $\phi \approx 1.27$, the jet speed is 43.1 m/s, and coflow speed is 0.8 m/s.

nanosecond repetitively pulsed discharges. In premixed flames, the discharges initiated combustion at high repetition rates of several tens of kilohertz. However, downstream propagation of the combustion occurred very close to the known flammability limit. In jet diffusion flames, discharge plasma stabilization was found to be best when the discharge is located where the mixture is in a combustible condition. The stabilization mechanism was found to be that in which the initiated combustion at the discharge location propagates along the combustible mixture contour, making the flames appear like an obliquely cut turbulent jet diffusion flame.

Acknowledgments

This work is supported by the National Science Foundation and the Department of Energy through the NSF/DOE Partnership in Basic Plasma Science. Partial support for M.S. Bak is provided through a Stanford Graduate Fellowship.

References

[1] A. Starikovskiy, N. Alexsandrov, Prog. Energy Combust. Sci. 39 (2013) 61–110.
[2] N.L. Aleksandrov, S.V. Kindysheva, I.N. Kosarev, S.M. Starikovskaia, A.Yu. Starikovskii, Proc. Combust. Inst. 32 (2009) 205–212.
[3] A. Bao, Y.G. Utkin, S. Keshav, G. Lou, I.V. Adamovich, IEEE Trans. Plasma Sci. 35 (2007) 1628–1638.
[4] G. Pilla, D. Galley, D.A. Lacoste, F. Lacas, D. Veynante, C.O. Laux, IEEE Trans. Plasma Sci. 34 (2006) 2471–2477.
[5] S.V. Pancheshnyi, D.A. Lacoste, A. Bourdon, C.O. Laux, IEEE Trans. Plasma Sci. 34 (2006) 2478–2487.
[6] W. Kim, M.G. Mungal, M.A. Cappelli, Combust. Flame 157 (2010) 374–383.
[7] M.S. Bak, H. Do, M.G. Mungal, M.A. Cappelli, Combust. Flame 159 (2012) 3128–3137.
[8] G.D. Stancu, F. Kaddouri, D.A. Lacoste, C.O. Laux, J. Phys. D: Appl. Phys. 43 (2010) 124002.
[9] M.S. Bak, W. Kim, M.A. Cappelli, Appl. Phys. Lett. 98 (2011) 011502.
[10] E.I. Mintoussov, S.J. Pendleton, F.G. Gerbault, N.A. Popov, S.M. Starikovskaia, J. Phys. D: Appl. Phys. 44 (2011) 285202.
[11] A.A. Nikipelov, A.E. Rakitin, I.B. Popov, G. Correale, A.Yu. Starikovskii, in: 49th AIAA Aerospace Sciences Meeting Including the New Horizons Forum and Aerospace Exposition, 4–7 January, Orlando, Florida. AIAA 2011-1214, 2011.
[12] W. Kim, H. Do, M.G. Mungal, M.A. Cappelli, IEEE Trans. Plasma Sci. 34 (2006) 2545–2551.
[13] W. Kim, H. Do, M.G. Mungal, M.A. Cappelli, Combust. Flame 153 (2008) 603–615.
[14] K. Criner, A. Cessou, J. Louiche, P. Vervisch, Combust. Flame 144 (2006) 422–425.
[15] H. Do, M.A. Cappelli, M.G. Mungal, Combust. Flame 157 (2010) 1783–1794.
[16] H. Do, S. Im, M.A. Cappelli, M.G. Mungal, Combust. Flame 157 (2010) 2298–2305.
[17] J. Kiefer, J.W. Tröger, Z.S. Li, M. Aldén, Appl. Phys. B 103 (2011) 229–236.
[18] H.F. Coward, G.W. Jones, US Bureau of Mines, Bulletin 503, 1952.
[19] D. Han, M.G. Mungal, Combust. Flame 124 (2001) 370–386.
[20] L. Muñiz, M.G. Mungal, Combust. Flame 111 (1997) 16–30.